Proceedings of the 2003 IEEE International Frequency Control Symposium and PDA Exhibition
Jointly with the 17th European Frequency and Time Forum

High-Spectral-Purity Microwave Oscillator: Design Using Conventional Air-Dielectric Cavity[1]

A. Sen Gupta[*], D. A. Howe[**], C. Nelson[**], A. Hati[+], F. L. Walls[#], and J. F. Nava[#]
* National Physical Laboratory, New Delhi, India
** National Institute of Standards & Technology, Boulder, CO, USA
+ NIST Guest Researcher, Burdwan University, Calcutta, India
# Total Frequency, Boulder CO, USA

Abstract - **We report exceptionally low PM and AM noise levels from a microwave oscillator that uses a conventional air-dielectric cavity resonator as a frequency discriminator. Our approach is to increase the discriminator's intrinsic signal-to-noise ratio by use of a high-power carrier signal to interrogate an optimally coupled cavity, while the high-level of the carrier is suppressed before the phase detector. We developed and tested an accurate model of the expected PM noise that indicates, among other things, that a conventional air-dielectric resonator of moderate Q will exhibit less discriminator noise in this approach than do more esoteric and expensive dielectric resonators tuned to a high-order, high-Q mode and driven at the dielectric's optimum power.**

I. INTRODUCTION

Microwave oscillators of the highest spectral purity usually employ frequency-locking to a high-Q resonance cavity to clean up the broadband phase noise [1-6]. The resonance cavity could be a part of the oscillator itself as its frequency-determining element [5, 6] or could be an external one, used only to stabilize the oscillator [2, 4]. In either case, it is used primarily as a discriminator. At microwave frequencies, any enhancement of the low-noise discriminator's sensitivity directly translates into corresponding improvement in the higher free-running oscillator's phase noise.

Several key aspects controlling the cavity discriminator sensitivity have been addressed extensively by earlier work. The most important one among these consists of increasing the cavity Q. Commonly, high-Q resonators employ use the whispering-gallery modes in Sapphire-Loaded Cavities (SLC). The unloaded Q varies from 2×10^5 to several million in going from the room temperature to cryogenic temperatures [3, 7]. The other key aspect controlling the discriminator sensitivity relates to the degree of suppression of the carrier signal reflected from the cavity, as this reduces the effective noise temperature of the nonlinear mixer, which acts as the phase detector. The amount of carrier suppression can be increased by making the effective coupling coefficient into the cavity approach its critical value of unity [3] and also by using interferometric signal processing [5, 6]. SLC resonators are commonly used with effective coupling coefficients near 0.7. Additional use of interferometric suppression can result in an overall carrier suppression of greater than 80 dB [5, 6].

Another important aspect of the discriminator sensitivity is that it scales directly as the power of oscillator signal incident into the cavity. This point has not been the subject of much discussion or experimental investigation. This is because when using an SLC resonator one is faced with the following problem. For a nearly critically coupled cavity, most of the incident microwave power is dissipated in the dielectric material due to high field confinement in a whispering-gallery mode. Due to the dependence of the dielectric permittivity of sapphire on temperature, fluctuations of the dissipated power, caused by Amplitude Modulation (AM) noise on the signal, give rise to SLC resonance frequency fluctuations. This effect of power to frequency conversion results in a discriminator noise floor that scales as the square of the dissipated power [8]. Thus increasing the power to improve the discriminator sensitivity can become counterproductive in the case of the SLC resonator. Suggested ways around this problem are: (a) frequency-temperature compensation of the sapphire dielectric resonator [9]; (b) suppression of the oscillator AM noise; and (c) controlling the SLC operating temperature by making use of the difference in frequency-temperature coefficients of different modes of the SLC resonator [8]. Frequency-temperature compensation for sapphire has been found to work effectively only at cryogenic temperatures. At room temperatures it is associated with relatively large loss of resonator Q.

In the present work we describe the design of a Cavity-Stabilized Oscillator (CSO) that uses a discriminator comprised of a room-temperature air-dielectric cavity at 10 GHz to clean up the phase noise of a commercial yttrium iron garnet (YIG) oscillator. Salient features of our design include (a) modest unloaded cavity Q values around 50,000-70,000; (b) coupling coefficient of approximately 0.95, achieved using simple coupling loops; (c) interferometric signal processing resulting in an overall carrier suppression of about 90 dB, and (d) incident signal power of +33 dBm. It has been demonstrated by a comprehensive theoretical model of the discriminator noise floor that the loss of sensitivity resulting from the lower values of Q are compensated by the large power level. Phase noise measurements on a fabricated prototype of the CSO, relative to two room-temperature SLC

[1] Contribution of U. S. Government, not subject to copyright. U. S. Government patent applied for.

Oscillators [10] in a three-cornered-hat configuration indicate that the approach presented here significantly improves on traditional CSO methodology that was originally developed at NIST [2].

II. DESCRIPTION OF OSCILLATOR

The basic approach in our experimental setup, shown in Figure 1, consists of cleaning up the phase noise of a YIG oscillator by using a high Q air-dielectric cavity as a discriminator. The YIG oscillator at 10GHz is a commercial one that allows voltage tuning over a ± 1 GHz range. Also, a special design enables very fast tuning with a 3 dB bandwidth of typically 2.5 MHz. Its output power of +13 dBm is amplified to +33 dBm using two stages of amplification.

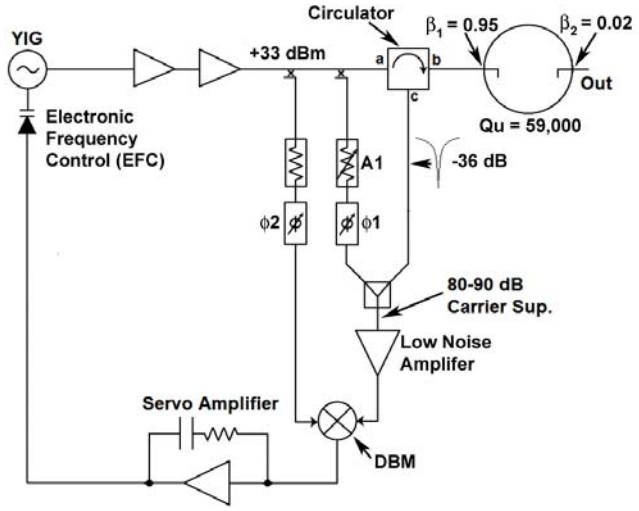

Figure 1: Schematic diagram of Cavity Stabilized Oscillator (CSO) as used in this paper.

The key element of the discriminator, the microwave cavity, is an air-filled cylindrical cavity operating in one of the higher TE modes. The inside surface of the cylinder and the end plates are highly polished and silver-plated. The dimensions of the cylinder are optimised to yield the highest value of Q. Two cavities have been fabricated to operate in TE023 and TE025 modes, and their unloaded Q values are measured to be 59,000 and 73,000, respectively.

Signal is coupled into and out of the cavity using small loops on the end plates, with their planes aligned with the radial plane of the cylinder. At this high frequency the loop diameters are barely over a millimetre. The coupling coefficient can be varied quite easily by just pushing the loops in and out by small amounts. The input probe, which is slightly larger in size, is adjusted to give a coupling coefficient of 0.95. The coupling of the output probe on the other hand is kept at only 0.02. Using the standard formulae for the reflection and transmission coefficients at the cavity resonance frequency

$$S_{11} = \frac{1-\beta_1+\beta_2}{1+\beta_1+\beta_2} \quad \text{and} \tag{1a}$$

$$S_{21} = \frac{2\sqrt{\beta_1 \cdot \beta_2}}{1+\beta_1+\beta_2}, \tag{1b}$$

we get a suppression of the reflected and the transmitted signal out of the cavity by 33 dB and 20 dB respectively. Considering that our input signal to the cavity has a power of +33 dBm, we get an output power of +13 dBm, which is high enough to be used without any further amplification. The advantage of using the transmitted output is that it results in additional filtering of the broadband noise and spurs. The entire cavity setup is mounted inside a thermally insulated enclosure and its temperature is controlled to within 10 mK.

Further suppression of the reflected signal is carried out using interferometric processing as shown in Figure 1. Using mechanically variable attenuator A1 and phase shifter ϕ1 to generate the compensating signal, it is possible to easily achieve further suppression of the reflected signal by 50 dB or more. The variable attenuator and the phase shifters are not kept under tight temperature control as the cavity. However, it is seen that this does not impair the carrier suppression settings very significantly over time. After suppression an input carrier level of about -50 dBm appears as input to the amplifier. This is low enough that it does not effectively contribute any low frequency flicker noise [5]. The amplifier has a gain of 30 dB and a noise temperature of about 100 K. The amplified output is supplied to one port of the phase detector, a double-balanced mixer (DBM), and the other port is given a reference signal in phase quadrature with the first. Phase quadrature condition can be easily obtained within an error of 1-2° using the mechanically-variable phase shifter ϕ2. This ensures that the YIG oscillator AM noise to phase noise conversion is not a significant factor compared to the thermal noise floor.

Finally the servo loop is completed by amplifying the phase detector output by the servo amplifier and feeding it to the voltage tuning port of the YIG. The servo amplifier is a two-stage integrator with additional high-frequency compensation, to give a unity-gain bandwidth of about 4 MHz. The high-frequency compensation is needed in order to offset the roll-off of the voltage tuning response of the YIG beyond about 1 MHz with a 3 dB point at 2.5 MHz.

III. OSCILLATOR PM NOISE MODEL

As mentioned earlier, the CSO consists of a YIG oscillator whose output is amplified and applied to a coupling port of the discriminator cavity through a circulator. The reflected signal out of the cavity comes out of the port C of the

circulator and is already highly suppressed since the coupling is very nearly critical. A portion of the input signal, adjusted to be of the same amplitude and opposite phase as the reflected signal, is combined with the reflected signal to suppress the carrier still further to about -50 dBm. This constitutes the so-called interferometric signal processing [5]. The highly suppressed signal is then amplified by the low noise amplifier before being applied to one port of the DBM. As a result of the very high level of carrier suppression, the amplifier output exhibits almost no flicker noise. The DBM acts as a phase detector whose other port has a portion of the input signal adjusted to be in phase quadrature with the reflected signal. By having the amplifier before the mixer, the effective noise contribution from the mixer is dominated by the amplifier gain and becomes relatively insignificant. The phase-detector output is the error signal that tracks the frequency fluctuations of the YIG oscillator relative to the cavity. This is applied to the voltage-control input of the YIG through the servo amplifier to stabilise its frequency.

The reflection coefficient of the signal incident on the cavity is given by

$$\Gamma = S_{11} = \frac{(1-\beta_e{}^2 + \Delta\nu'^2) + j(2\cdot\Delta\nu'\cdot\beta_e)}{(1+\beta_e)^2 + (\Delta\nu'^2)}\ , \qquad (1c)$$

where

$\beta_e = \dfrac{\beta_1}{1+\beta_2}$, the effective coupling coefficient,

$\Delta\nu' = \dfrac{\nu-\nu_{res}}{HUB} = \dfrac{\Delta\nu}{HUB}$, and

$HUB = \dfrac{\nu_{res}}{2\cdot Q_u}$, the half unloaded bandwidth.

ν, ν_{res} and Q_u are respectively the carrier frequency of the signal, the cavity resonance frequency, and the unloaded cavity Q. Further if the reflected signal is applied to the RF port of the DBM and a reference signal in phase quadrature to its LO port, we can show that the DBM output is

$$v_o = k_d\cdot\sqrt{P_i}\cdot(\mathrm{Im}\,\Gamma) = k_d\cdot\sqrt{P_i}\cdot\frac{2\cdot\beta_e}{(1+\beta_e)}\cdot\frac{1}{\left\{1+\left(\frac{\Delta\nu}{HLB}\right)^2\right\}}\cdot\frac{\Delta\nu}{HLB}\ , \quad (2)$$

where P_i, k_d and $HLB = (1+\beta_e)$ are respectively the incident signal power, DBM conversion gain and cavity half loaded bandwidth. The corresponding signal power out of the DBM is

$$SP_0 = k_d{}^2\cdot P_i\cdot\frac{4\cdot\beta_e{}^2}{(1+\beta_e)^2}\cdot\frac{1}{\left\{1+\left(\frac{\Delta\nu}{HLB}\right)^2\right\}^2}\cdot\left(\frac{\Delta\nu}{HLB}\right)^2. \qquad (3)$$

We further make use of the relationship that connects the phase-noise spectral density $S_\varphi(f)$ as a function of the Fourier frequency f and the corresponding frequency fluctuation $\Delta\nu$ of the signal, whose rms value is denoted by $\Delta\nu_{rms}$, as [11]

$$S_\varphi(f) = \left(\frac{\Delta\nu_{rms}}{f}\right)^2 \quad \text{or} \quad \left(\Delta\nu_{rms}\right)^2 = f^2\cdot S_\varphi(f). \quad (4)$$

We note that if the YIG oscillator is locked to the cavity so that its carrier frequency is ν_{res}, then phase noise induced $\Delta\nu$ in (4) has the same meaning as in (3). Thus, combining (3) and (4), we can write the rms power out of the DBM as

$$SP_{0rms} = k_d{}^2\cdot P_i\cdot\frac{4\cdot\beta_e{}^2}{(1+\beta_e)^2}\cdot\frac{1}{\left\{1+\left(\frac{f^2\cdot S_\varphi(f)}{HLB^2}\right)\right\}^2}\cdot\left(\frac{f^2\cdot S_\varphi(f)}{HLB^2}\right) \quad (5)$$

which can be rewritten simply as

$$SP_{0rms} = k_d{}^2\cdot P_i\cdot\frac{4\cdot\beta_e{}^2}{(1+\beta_e)^2}\cdot\left(\frac{f^2\cdot S_\varphi(f)}{HLB^2}\right) \quad (6)$$

since $S_\varphi(f) << 1$ for a reasonable low-noise oscillator.

To compute the discriminator noise floor, we need to consider the noise power present at the output of the DBM due to different sources. The major source is the thermal noise of the microwave amplifier. As mentioned earlier, the flicker noise of the amplifier is very small since the carrier is very highly suppressed and the noise of the DBM is swamped by the amplifier gain. We can write the noise contribution of the amplifier and other lossy components of the system as

$$N_{amp} = k_d{}^2\cdot k_B\cdot(T_{amp} + T_0) \quad (7)$$

Where T_{amp} is the effective noise temperature of the amplifier, T_0 is the ambient temperature (300 K), and k_B is Boltzmann's constant. The second source of noise is the ferrite circulator, which lies within the discriminator. In absolute terms its phase noise is quite small and can be expressed in the form (for each of its three segments) [6]

$$S_{\varphi}^{circ}(f) = -150 - 12\log_{10}(f)\ \text{dBc/Hz}\,. \quad (8)$$

Referring to Figure 1, the expression for the noise contributed to the discriminator by the segment a-b of the circulator is similar to that from the oscillator, as given in (6):

$$N_{circ(a-b)} = k_d{}^2 \cdot P_i \cdot \frac{4\cdot\beta_e{}^2}{(1+\beta_e)^2} \cdot \left(\frac{f^2 \cdot S_{\varphi}^{circ(a-b)}(f)}{HLB^2} \right). \quad (9)$$

However, the noise contributed by the segment b-c modulates a much suppressed carrier of the signal reflected from the cavity. This can be written as

$$N_{circ(b-c)} = k_d{}^2 \cdot P_i \cdot \frac{(1-\beta_e)^2}{(1+\beta_e)^2} \cdot S_{\varphi}^{circ(b-c)}. \quad (10)$$

The third source of noise is the phase shifter, which is used to adjust the phase of the compensating signal to exactly oppose the reflected signal and interferometrically cancel it. To make the cancellation automatic it is usual to use a voltage-controlled ferrite phase shifter (VCP). Although in our experimental setup we have used only a mechanical phase shifter, which does not produce any significant phase noise, we include the discussion of the VCP for the sake of completeness. The noise model for a typical VCP is [6]

$$S_{\varphi}^{vcp}(f) = -147 - 7.5\log_{10}(f)\ \text{dBc/Hz}. \quad (11)$$

The noise contributed by the VCP also modulates the suppressed reflected carrier, and the expression for it is similar to that for the circulator segment b-c. We can write this as

$$N_{vcp} = k_d{}^2 \cdot P_i \cdot \frac{(1-\beta_e)^2}{(1+\beta_e)^2} \cdot S_{\varphi}^{vcp}. \quad (12)$$

Thus the noise floor of the discriminator can be computed simply by realising that it is the smallest signal power out of the DBM, given by (6), which equals the sum of all the noise contributions from different sources, given by (9), (10), and (12):

$$SP_{0rms} = N_{amp} + N_{circ(a-b)} + N_{circ(b-c)} + N_{vcp}. \quad (13)$$

Substituting from (6), (9), (10), and (12), we get the noise floor S_{φ}^{nf} for the discriminator as

$$S_{\varphi}^{nf} = \frac{k_B(T_{amp}+T_0)}{P_i} \cdot \frac{(1+\beta_e)^2}{4\beta_e} \cdot \left(\frac{HLB}{f}\right)^2 + S_{\varphi}^{circ}(f) + \left\{ \frac{(1-\beta_e)^2}{4\beta_e{}^2} \cdot \left(\frac{HLB}{f}\right)^2 \right\} [S_{\varphi}^{circ}(f) + S_{\varphi}^{vcp}(f)]\,. \quad (14)$$

The first term in (14) corresponds to the microwave amplifier, and the second and third correspond to the circulator and VCP.

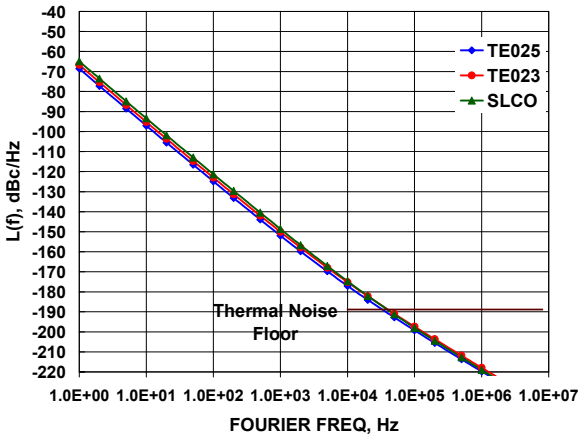

Figure 2: The computed discriminator noise floors for the CSO using TE023 and TE025 cavities and the SLCO of Tobar et al. [7].

IV. MEASURED PM NOISE OF THE CSO

Before describing the experimental results, we discuss the expected noise performance of the CSO based on our noise model of the previous section. Computations of the expected noise floor were made using (14) with different parameters in our experimental setup. The parameters considered are: ν_{res} = 10 GHz; Q_u = 73,000 (TE025) and 59,000 (TE023); β_1 = 0.95; β_2 = 0.02; P_i = +33 dBm. We also account for the circulator and the VCP noise. Although a VCP has not been used in our prototype CSO, including it will enable a comparison with the earlier results with the SLCO [7]. The computed noise floors for the TE023 and TE025 cavities shown in Figure 2 indicate that results of the two cavities are not markedly different. This is expected since there is a difference of only 20 % between their $Q_u$values. The noise floor initially falls off as f^{-3} and gradually tapers off to a f^{-2} behavior beyond 2 kHz. Beyond 50 kHz the noise floor drops below -190 dBc/Hz, which is the thermal noise floor for the given signal level. Thus we would expect the CSO output to be at the thermal noise level beyond 50 kHz. For the sake of comparison, we have also shown in Figure 2 the computed noise floor using (14) for the SLCO case by Tobar et al. [7]. The parameters considered are: ν_{res} = 10 GHz, Q_u = 190,000, β_1 = 0.75, β_2 = 0.15, P_i = +17 dBm, and we also include the

noise contributions of the circulator and VCP. We clearly observe that the noise floors in the present results are about 2 to 3 dB lower than for the SLCO throughout the entire range of Fourier frequencies. This is a very significant conclusion, indicating that even using relatively lower-Q air-dielectric cavities it is possible to achieve less discriminator noise than in the SLCO just by driving it with very high signal power. To lend credibility to our model computations we observe that the experimental results of Tobar et al. [7] match the SLCO noise floor in Figure 2 within a few dB between 10 Hz and 5 kHz. Above this frequency, their observed noise increases due to insufficient servo gain.

Since a VCP has not been used in our experiment, it is of interest to determine the discriminator noise floor by not including its contribution in (14). This is shown in Figure 3 for the TE023 and TE025 cavities with the same parameters as in Figure 2, while the SLCO noise floor is shown, as before, for comparison. We observe a significant lowering of the noise floor, which is lowered as much as 7 to 9 dB between 1 kHz and 100 kHz. Also apparent is a f^{-3} slope of the noise floor below 200 Hz, due predominantly to the contribution of the circulator's noise, which can be reduced by making the value of β_1 closer to unity. It can be shown that by making $\beta_1 = 0.98$, there is a reduction of nearly 5 dB at 1 Hz. Above about 200 Hz the noise floor follows a f^{-2} slope as its value becomes directly proportional to the thermal noise of the microwave amplifier and square of the cavity Q, and inversely proportional to the input power.

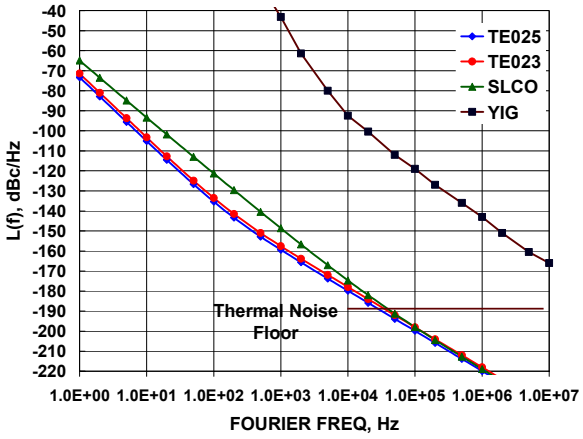

Figure 3: Computed discriminator noise floors as in Figure 2, but not including the VCP contribution for the CSO. Also shown is the measured PM noise of the free-running YIG oscillator used in the CSO.

The PM noise of the YIG oscillator used in our setup is quite large compared with the discriminator noise floor, which is our goal for the CSO. We have experimentally determined the free-running YIG noise using a delay-line discriminator technique [10] in order to estimate the servo gain needed to bring it down to the discriminator noise floor. These results are also shown in Figure 3. The need for very high servo gain is clearly apparent. At 100 kHz and 1 kHz the needed gains are respectively about 84 dB and 115 dB. Such high gains have been achieved in the CSO by cascading two integrators.

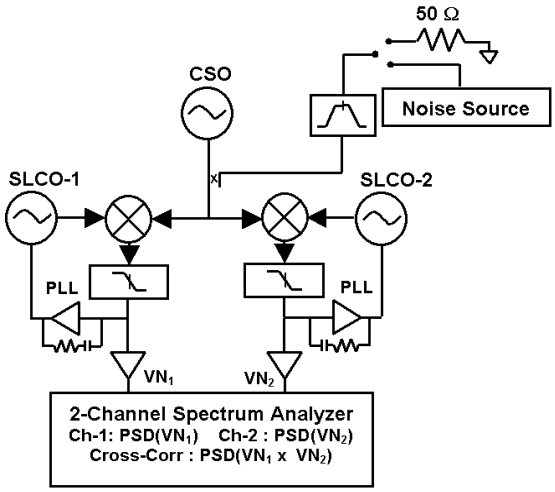

Figure 4: Cross-correlation three-cornered-hat experimental setup for measurements of PM noise of the CSO.

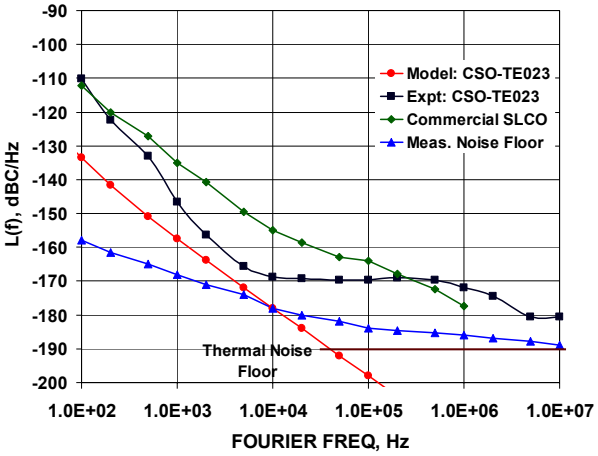

Figure 5: Measured PM of the CSO using a TE023 cavity. Also shown are the discriminator noise floor as in Figure 3 and the measured PM noise of an SLCO.

The experimental setup shown in Figure 4, for the measurement of the PM noise of the CSO, is a cross-correlation setup that uses two commercial SLCOs [11] as reference oscillators in a three cornered hat configuration [10]. Care was taken to eliminate or minimize the level of cross talk between the three oscillators by using adequate isolation between them. Using the setup in Figure 4 it was possible to get a measurement noise floor that almost reached the thermal floor near 10 MHz.

Figure 5 shows the observed PM noise of the CSO, and for comparison the computed discriminator noise floor using the TE023 cavity. Also shown is the noise floor of the measurement system. Best agreement between the CSO and our model computation happens between 1 to 10 kHz, where it is within 6 to 9 dB. At higher Fourier frequencies up to about 1 MHz the disagreement increases because of the gradual roll-off of the integrator in the servo. Beyond 1 MHz the drop in the CSO noise is caused by the band-pass filter action of the cavity. For Fourier frequencies lower than 1 kHz, the PM noise of the CSO begins to deviate by more than 10 dB from the computed discriminator noise, becoming 20 dB worse at 100 Hz. In the low-frequency range there are two major factors that play a role. Firstly, due to inadequate stability of the temperature controller, the fluctuations of the ν_{res} of the cavity translate into increased PM noise of the CSO. This can be reduced with improved temperature control, which we plan to do in the future.

Secondly, spurious low-frequency peaks, which were apparent in the raw data consisting of both electromagnetic pickup and mechanical resonances, degrade the CSO noise. The effect of these should be reduced with better mechanical mounting and isolation. Finally we have shown the PM noise of one of the commercial SLCO's [11] that was used in our cross-correlation PM noise-measurement setup. Clearly, even in its preliminary implementation the CSO exhibits significantly lower noise than the SLCO.

VI. FUTURE PROSPECTS

The present results of the low-phase-noise behavior of the CSO employing an air-dielectric over-moded cavity are very encouraging. However, the present work is preliminary and will need to be refined in order to approach the noise predicted by the model computations. In the future, we plan to work further on the following aspects:

(a) More rigid mounting and environmental isolation of the cavity
(b) More stable mounting of the coupling loops
(c) Better temperature control
(d) Higher-gain servo with higher-frequency unity-gain point
(e) Choice of higher carrier frequency for the CSO
(f) Use of a 3 dB hybrid in place of the circulator.

VI. SUMMARY

We have described the construction of a cavity-stabilised oscillator (CSO) that uses a conventional air-dielectric microwave cavity resonator as a frequency discriminator to drastically lower the free-running phase noise of a commercial YIG oscillator. The novelty of our approach is that it aims to offset the disadvantage of a modest cavity Q of about 70,000 (compared to the more esoteric and expensive SLC systems, both at room and cryogenic temperatures) by increasing the carrier power to interrogate an almost critically coupled cavity. We have developed and tested an accurate model of the expected phase noise, which indicates that the CSO performance should indeed compare well with that of the SLCO. Our initial measurements on the first prototype CSO show a phase noise of -105 dBc/Hz at 100 Hz, -145 dBc/Hz at 1kHz, and -178 dBc/Hz at 1 MHz offset from the carrier. We suspect that the lower-frequency results are contaminated by inadequate environmental isolation, while the high-frequency end is compromised by lack of servo gain. In the future we propose to further refine the noise performance of the CSO by addressing the above aspects and possibly also using higher carrier frequencies.

ACKNOWLEDGEMENTS

We thankfully acknowledge very useful discussions with Eugene Ivanov.

REFERENCES

[1] Panov V. I. and Stankov P. R., Frequency Stabilisation of Oscillators with high-Q leucosapphire dielectric resonators, Radiotechnika I Electronika **31**, 213, (1986)

[2] Walls F. L., Felton C. M. and Martin T. D., High Spectral purity X-Band Source, IEEE Freq Control Symp. Proceedings, **44**, 542-547, (1990)

[3] Dick G. J. and Santiago D., Microwave Frequency Discriminator with a cryogenic sapphire resonator for ultra-low phase noise, IEEE Freq Control Symp. Proceedings, **46**, 176-182 (1992)

[4] Santiago D. and Dick G. J., Closed loop Tests of the NASA Sapphire Phase Stabiliser, IEEE Freq Control Symp. Proceedings, **47**, 774-778 (1993)

[5] Ivanov E. N., Tobar M. E. and Woode R. A., Advanced Phase Noise Suppression technique for the next generation of Ultra-Low Noise Microwave Oscillators, IEEE Freq Control Symp. Proceedings, **49**, 314-320 (1995)

[6] Ivanov E. N., Tobar M. E. and Woode R. A., Applications of Interferometric Signal Processing to Phase Noise Reduction in Microwave Oscillators, IEEE Trans on MTT, **46**, No 10, 1537-1545 (1998)

[7] Tobar M. E., Ivanov E. N., Woode R. A. and Searles J. H., Low Noise Microwave Oscillators based on High-Q

Temperature stabilized Sapphire Resonators, IEEE Freq Control Symp. Proceedings, **48**, 433-440 (1994)

[8] Ivanov E. N., Tobar M. E., Future Trends in the Development of Ultra-Low Noise Microwave Oscillators with Interferometric Signal Processing, Joint meeting of EFTF and IEEE FCS Proceedings, **53**, 552-556 (1999)

[9] Hartnett J. G., Tobar M. E., Mann A. G., Ivanov E. N. and Krupka J., Frequency-Temperature Compensation in Ti^{3+} and Ti^{4+} doped sapphire whispering gallery mode resonators, IEEE Freq Control Symp. Proceedings, **52**, 512-517 (1998)

[10] Sullivan D.B., Allan D.W., Howe D.A., and Walls F.L. (Editors), "Characterization of Clocks and Oscillators", National Institute of Standards and Technology Technical Note 1337, March 1990.

[11] Poseidon Scientific Instruments Pty Ltd**,** 1/95 Queen Victoria Street, Fremantle WA 6160 (AUSTRALIA). For completeness, commercial products are mentioned in this document. No endorsement is implied. Products are available from other manufacturers.